



## WP1 summary report relevant for risk assessment

---

### Deliverable number 1.3

Jens Karstens<sup>1</sup>, Christian Berndt<sup>1</sup>, Stefan Bünz<sup>2</sup>, Alexandros Tasianas<sup>2</sup>, Holger Class<sup>3</sup>, Waqas Ahmed<sup>3</sup>, Bogdan Orlic<sup>4</sup>

<sup>1</sup> GEOMAR Helmholtz Centre for Ocean Research Kiel, Germany

<sup>2</sup> Department of Geology, University of Tromsø, Norway

<sup>3</sup> Department of Hydromechanics and Modelling of Hydrosystems, University of Stuttgart, Germany

<sup>4</sup> TNO, Centre for Earth, Environmental and Life Sciences, The Netherlands

Deliverable description: This report should summarize all information from WP1 relevant to assessing geological risks of CO<sub>2</sub> leakage at sequestration sites as input to CCT4

## Inhalt

Objectives.....	<b>Fehler! Textmarke nicht definiert.</b>
1. Geological risks for the submarine storage of CO <sub>2</sub> .....	3
1.1. Fluid pathways.....	3
1.1.1. Seismic chimneys and pipes .....	3
1.1.2. Faults .....	4
1.1.3. Seafloor features .....	5
1.2. Methods for surveying .....	7
1.2.1. Conventional 3D seismic data .....	7
1.2.2. P-cable 3D seismic data .....	8
1.2.3. Seafloor mapping .....	8
2. Risk Evaluation.....	10
2.1. Leakage Scenarios .....	10
2.1.1. Leakage along existing fluid conduits (fault and chimneys) (2 pages, GEOMAR) ..	<b>Fehler! Textmarke nicht definiert.</b>
2.1.2. Formation of focused fluid flow structures as the result of CO <sub>2</sub> storage .....	<b>Fehler! Textmarke nicht definiert.</b>
2.2. Generic chimney Simulations - Formation of focused fluid flow structures as the result of CO <sub>2</sub> storage .....	15
2.3. Fluid flow simulations of leakage along chimneys (Sleipner).....	10
2.4. Fluid flow simulations of leakage along a fault (Snøwhit).....	13
2.5. Geomechanical simulation .....	16
3. Summary and recommendations .....	20
5. References .....	22

## Aim of this report

This report summarizes all information from WP1 that are relevant for assessing geological risks for the leakage of CO<sub>2</sub> at sequestration sites and builds on deliverables D1.1 and D1.2. This report will be the input for CCT4 “Framework of Best Environmental Practices in the Management of Offshore CO<sub>2</sub> Injection and Storage”.

## 1. Geological risks for the submarine storage of CO<sub>2</sub>

### 1.1. Fluid pathways

#### 1.1.1. Seismic chimneys and pipes

Seismic chimneys and pipes are vertical seismic anomalies interpreted as focused fluid flow structures, which hydraulically connect deeper stratigraphic layers with the overburden (Figure 1; Løseth et al., 2009; Cartwright et al. 2007). Their formation is generally believed to be controlled by overpressure-induced hydrofracturing of an impermeable sedimentary overburden (Løseth et al., 2009; Cartwright et al. 2007). The activity of vertical fluid conduits can be limited to blowout-like events or fluid flow may be continuous and long-lasting, e.g. the chimney structures above the leaking hydrocarbon reservoirs. The terms seismic chimney and pipe are used interchangeably in the literature. The scale of seismic chimney structures varies from meters to hundreds of meter in length and diameter. Seismic chimneys most likely represent a continuum of geological structures including gas filled fracture networks, the remnants of single pulse blowout-like gas expulsions and zones of sediment fluidization as the result of overpressure charged fluid flow. Each process has different implication on the hydraulic properties of an affected sedimentary overburden. While fracture networks most likely represent effective fluid pathways, structures associated with blowout-like events have probably been plugged by mobilized sediments after the formation.

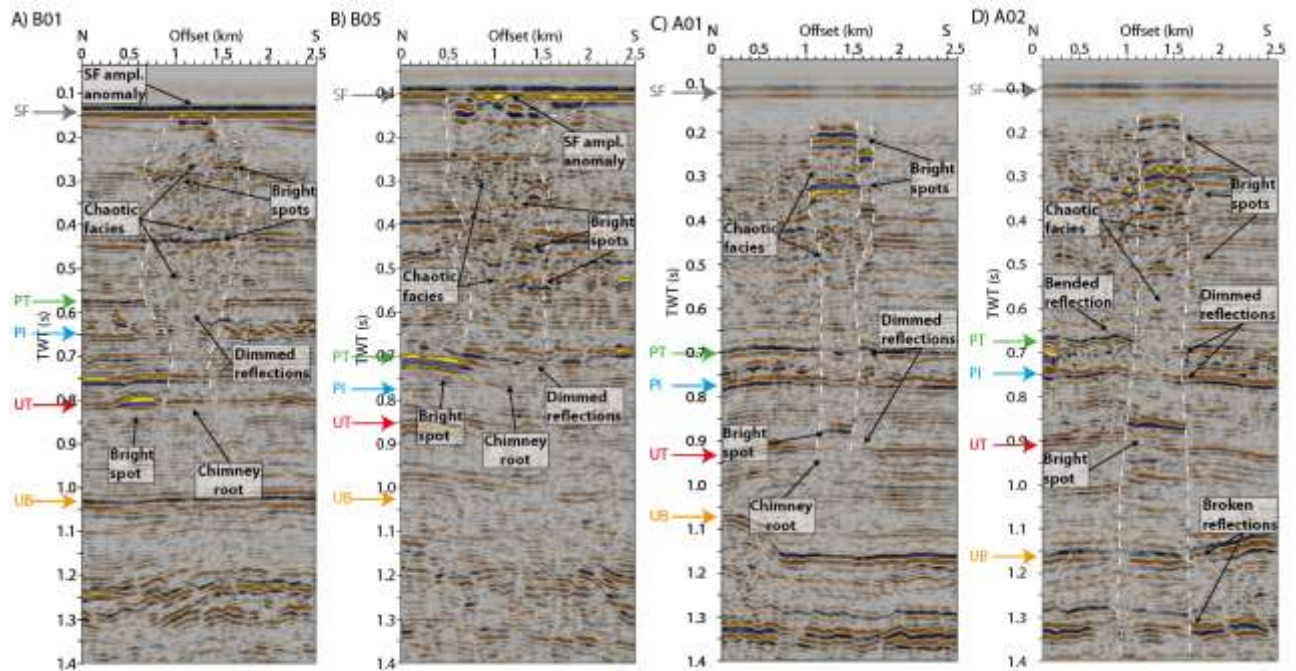


Figure 1: Seismic chimneys associated with gas-filled fracture-networks (A & B) and with rapid fluid release (C & D; Karstens and Berndt, 2015)

### 1.1.2. Faults

Faults represent areas of weakness with respect to geomechanical processes. We know that there are both permeable and impermeable faults in the study area that could present a potential geological risk (Løtveit et al., 2012; Ostanin et al., 2013; Ostanin et al., 2012). Typical permeabilities for low permeable fault zones are (0.00001mD - 0.0001mD) and for highly permeable damage zones (0.001mD - 10mD) (Mizoguchi et al., 2008; Moore et al., 2009). Permeabilities of single deformation bands vary in the range of 0.1 – 100mD (Rotevatn et al., 2013). In the simulations carried out as part of the ECO2 modelling activities for Snøhvit, two fault thicknesses are used (50m and 150m) and a fault permeability ranging over (0,0001, 1, 50, 100 and 300mD; Figure 2).

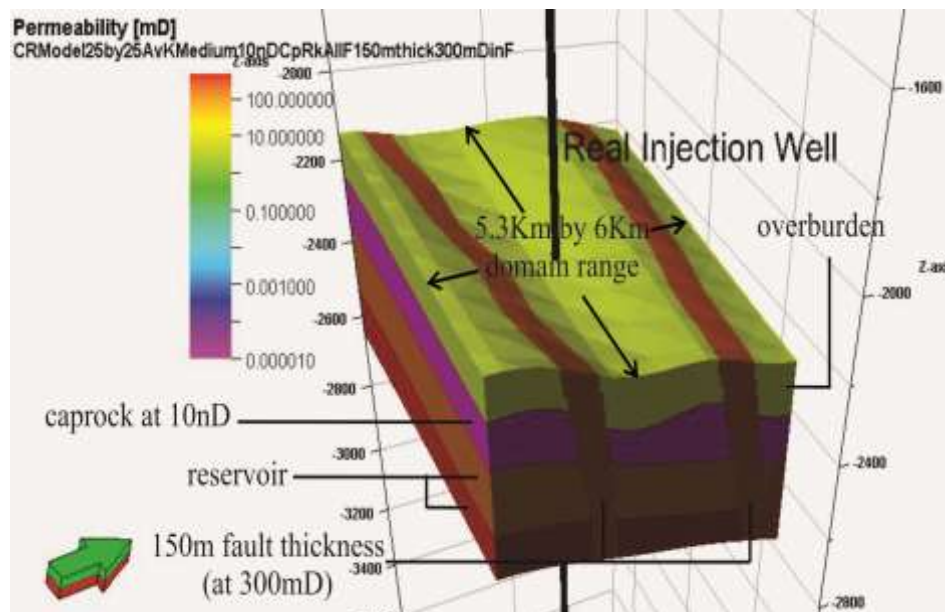


Figure 2: Permeability model for the faulted sedimentary cover scenario F7 (Medium background permeability, 150m fault thickness at 300mD)

The porosity is not varied in this study. For the background porosity, the values for the medium scenario (see MS12 geological models report) with a fault porosity of 18% are applied. 18% is the maximum value found in a core from the San Andreas Fault (Janssen et al., 2011).

### 1.1.3. Seafloor features

Up to now, preferentially seismic data sets were used to characterize the overburden over potential storage reservoirs. However, fractures in the seafloor are difficult to detect with the use of conventional 3D seismic. To reveal potential seafloor leakage structures in detail, the use of an autonomous underwater vehicle (AUV) equipped with a high-resolution interferometric synthetic aperture sonar system (HISAS – commercially available) is necessary. The HISAS is capable to obtain an image resolution of up to 5 x 5 cm and can thus observe diverse detailed features at the seafloor such as fractures or pockmarks.

Fractures in the seafloor can be connected to a complex fracture network in the subsurface and give rise to active fluid or gas flow from deep geological formations into the seawater. The most obvious indicators for fluid or gas flow from a fracture are the growth of bacterial mats or bubbles rising from the seafloor. Fractures can be characterized by linear, en echelon and branching segments as well as by ring structures (Figure 3). They can be several

ECO2 project number: 265847

Deliverable number 1.3, WP1, lead beneficiary no 1 (GEOMAR)

kilometers long and vary in width and form over the distance. Due to a lack of high resolution imaging data, it remains unclear how common fractures in the seafloor are.

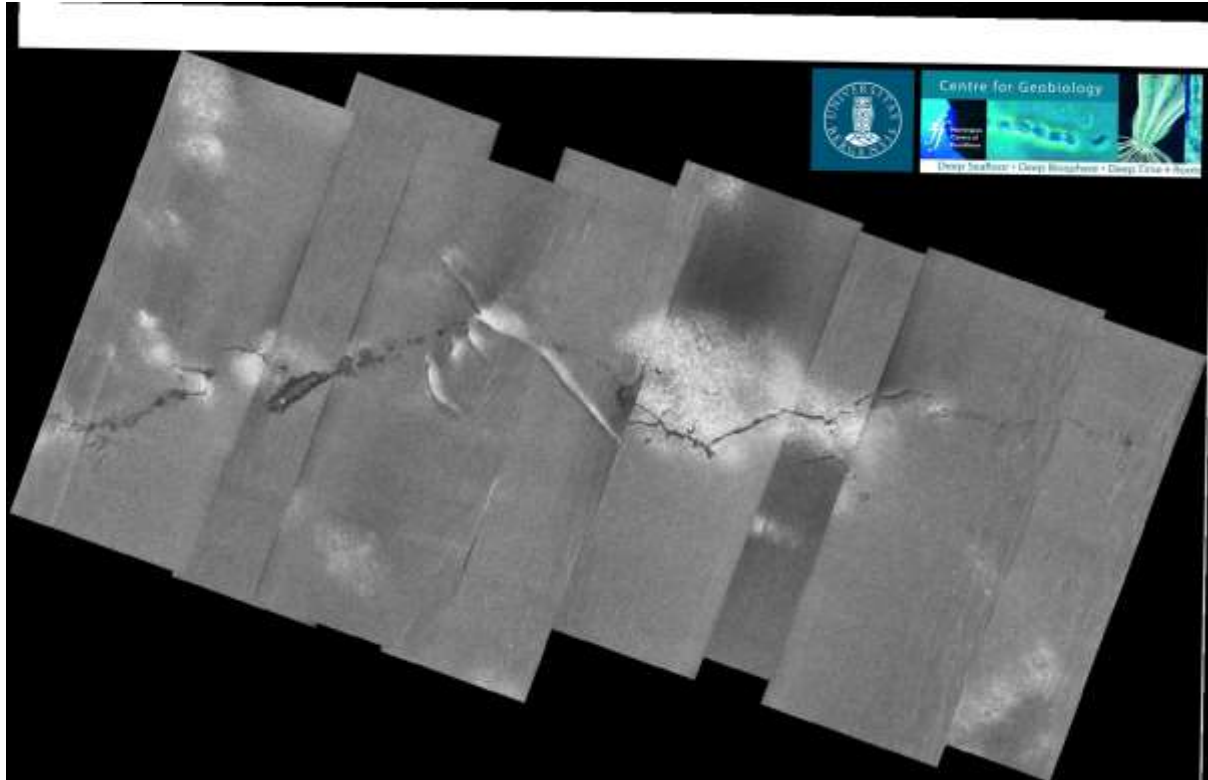


Figure 3: Central and eastern part of the Hugin Fracture, imaged by using the HISAS.

Pockmarks are other special features at the seafloor. Seabed fluid flow involving seepage of free methane gas and/or water with a high methane concentration in solution is found in every sea and ocean (Judd, 2003). Acoustic and seismic data can reveal seabed fluid flow indicators such as pockmarks, mud volcanoes, acoustic chimneys, pingos and authigenic carbonate build up which are related to hydrocarbon migration. Pockmarks correspond to erosive features formed by escape of gas and/or fluids from low-permeability, fine-grained surficial sediments.

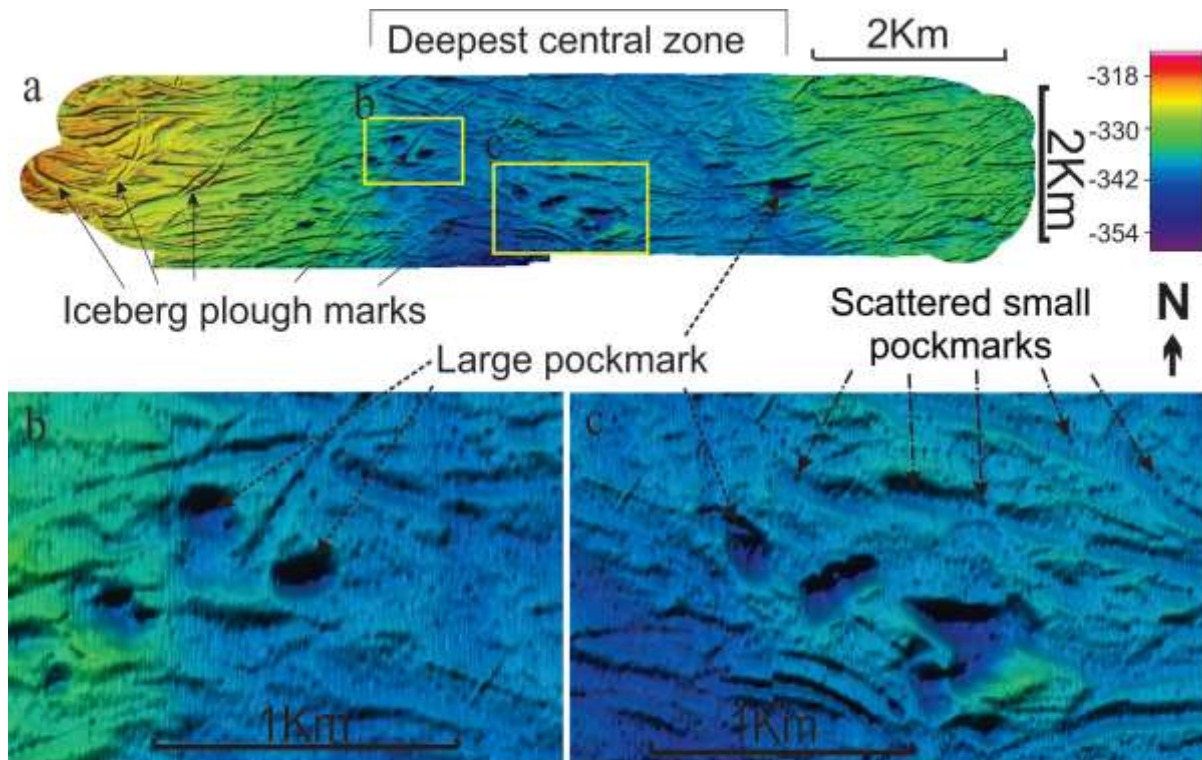


Figure 4: Pockmarks and plough marks at the seafloor of Snøwhit from P-cable seismic

## 1.2. Methods for surveying

### 1.2.1. Conventional 3D seismic data

2D seismic, 3D seismic and P-cable seismic all have their limitation in shallow water depths, i.e. 150 m and less. Special survey---design can improve the resolution in these cases only to some extent, whereas good processing, and especially the removal of seafloor multiples, is of crucial importance. Alternatively, seismic investigation should be complemented by sub-bottom profiling in order to fill the resolution gap around the seafloor. Conventional 3D seismic employed by the oil and gas industry consists of an acoustic source array and a multi-channel streamer array. It has already replaced 2D surveys as a standard in the industry, but it is a large-scale operation sometimes involving several vessels with streamers and acoustic sources. The survey design is usually optimized for reservoir depth, i.e. from 1000 m below seafloor (bsf), and therefore the receiver offset is equally large, up to 13 km. This also means that a velocity model for the subsurface is easily acquired with conventional 3D seismic acquisition. Today, many specialized survey designs are offered by different companies, involving not only streamer arrays but also ocean bottom cables (OBC) and ocean bottom nodes (OBN) as receivers. One clear advantage is the contact to the solid seafloor which enables recording of different types of acoustic waves, pressure and shear waves, which

**ECO2 project number: 265847**

**Deliverable number 1.3, WP1, lead beneficiary no 1 (GEOMAR)**

gives a better understanding of the subsurface and a clearer indication of fluid-filled compartments.

Seismic data is very sensitive for imaging seafloor parallel structures, but has however limitations in resolve vertical oriented structures. The seismic image of vertical conduits is therefore not very detailed. When interpreting seismic chimneys, it is important to rule out that the chimney itself is only a seismic artifact as the result of inadequate processing, data gaps or amplitude blanking beneath seismic anomalies. Only (repeated) 4D seismic monitoring allows a reliable evaluation of the interaction of CO<sub>2</sub> and a paleo fluid pathway.

### 1.2.2. P-cable 3D seismic data

The P-Cable high resolution system has proven useful for mapping fluid leakage systems, shallow gas and gas hydrates in order to better understand fluid flow processes (Petersen et al., 2010; Rajan et al., 2013). P-Cable high resolution seismic allows to focus on the top part of the subsurface and characterize in more detail shallow features as well as plough marks. The P-Cable 3D high-resolution seismic system consists of a seismic cable towed perpendicular (cross cable) to the vessel's steaming direction. An array of multi-channel streamers is used to acquire many seismic lines simultaneously, thus covering a large area with close in-line spacing in a cost efficient way. The cross-cable is spread by two paravanes that due to their deflectors attempt to move away from the ship. Due to the curvature of the cross cable, the streamers are closer together, i.e. in the range of 10-12 m. With the high resolution P-Cable system the temporal resolution is improved by 3-5 times and spatial resolution can be at least one order of magnitude higher than for conventional 3D seismic (Planke et al., 2009). The improved resolution allows for a better imaging of seabed structures such as pockmarks.

### 1.2.3. Seafloor mapping

Multibeam echosounders (MBES) and single-beam echosounders (SBES) are potent tools to image both the water column and seabed. SBES have been used for many years in fisheries research, and can be used to identify the presence/absence of bubbles within a typical 10 degree beam footprint. MBES systems are used to collect high-resolution seafloor profiles across a swath typically 2-2.5x the water depth. Multibeam systems can also be used to

**ECO2 project number: 265847**

**Deliverable number 1.3, WP1, lead beneficiary no 1 (GEOMAR)**

acquire water column information, giving the full 3d shape of rising bubble plumes and fish schools.

Bathymetry is typically collected using a MBES. The R/V G.O. Sars, R/V James Cook, and R/V Alkor have an EM302, EM710, and Seabeam 1000 respectively. All of these MBES systems are fully capable within the depth range of 100 m to 1000 m applicable to this project. Proper technique in acquisition, quality assessment, and processing is essential to the creation of an accurate MBES data product. The key factors contributing to a quality survey are: the sound velocity profile, monitoring of the acquisition software, and grid-wide crossing lines for syn-acquisition reference.

The most important factor in the collection of acoustic soundings is the sound velocity profile (SVP). The sound structure informs ray-tracing algorithms in the acquisition software, and is used in real-time to accept or reject soundings used by the bottom-lock algorithms. In the open ocean the SVP is relatively stable, and a single CTD or expendable bathythermograph (XBT) deployment at the beginning of a survey is more than sufficient to acquire quality data. In places with complex topography, especially in regions of high relief with respect to the surrounding terrain, the SVP may only be stable for a matter of hours. Knowledge of the region to be surveyed is essential to estimate the frequency of SVPs that will need to be collected.

## 2. Risk evaluation based on numerical simulations

### 2.1. Leakage scenarios

The evaluation of geological risks for the sub-seabed storage of CO<sub>2</sub> builds on a set of numerical simulation, which has been carried out in the framework of the ECO2 project. These simulations aim to quantify the risk of leakage of CO<sub>2</sub> for different scenarios, which have been summarized in D1.1 including the leakage through pre-existing fluid flow systems, through abandoned wells and the creation of a blowout.

During the ECO2 modelers meeting in Plymouth in March 2014, the project agreed on four leakage scenarios, which should be simulated in order to create first benchmark models with a priority on scenarios 1 and 2 (table 1).

Scenario	Max flux rate (at seafloor)	Footprint (at seafloor)	
1) Siesmic Chimney	~150T/d	500m diameter circle	
2) Fault/Fracture	~15T/d	200x2000m <sup>2</sup> fracture zone	
3) Blowout	~150T/d	50m diameter circle	
4) Well/borehole	~20T/a	few meters diameter	

Table 1: Leakage scenarios based on the March 2014 modelers meeting.

### 2.2. Fluid flow simulations of leakage along chimneys (Sleipner)

For the Sleipner CCS project we developed three different geological models, which include or exclude specific stratigraphic units depending on the scientific objectives. The first model does not includes the complete overburden or leakage structures and was used to define the permeability field by matching the modeled CO<sub>2</sub> plume shape with the real shape derived from time-lapse seismic data (figure 5).

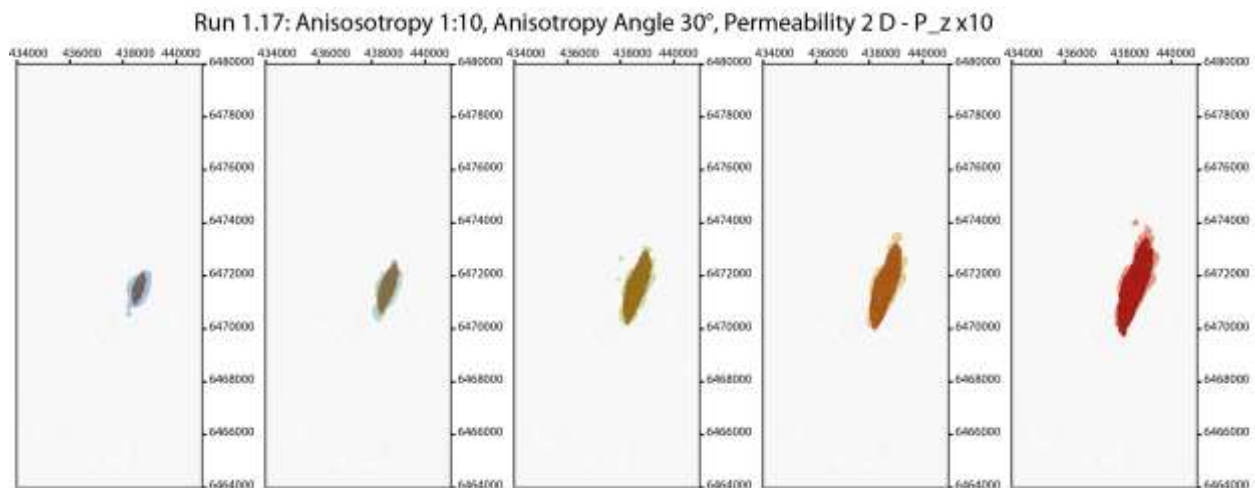


Figure 5: Plume comparison with seismic data for different time steps.

Based on the best plume shape, we have chosen the parameter for the simulations, which include the overburden and the chimneys. These simulations cover a time period of 200 years. The two most important simulations are the “realistic” case, which models 30 years of injection and include CO<sub>2</sub> dissolution and the “worst” case, which models 200 years of continuous injection neglecting CO<sub>2</sub> dissolution.

Figure 6 shows the CO<sub>2</sub> plume extent of the “realistic” case for 30, 50, 100 and 200 years. The most important outcome is that the growth of the CO<sub>2</sub> plume slows down significantly after stopping the injection and that the CO<sub>2</sub> will not reach the chimney structures under realistic conditions.

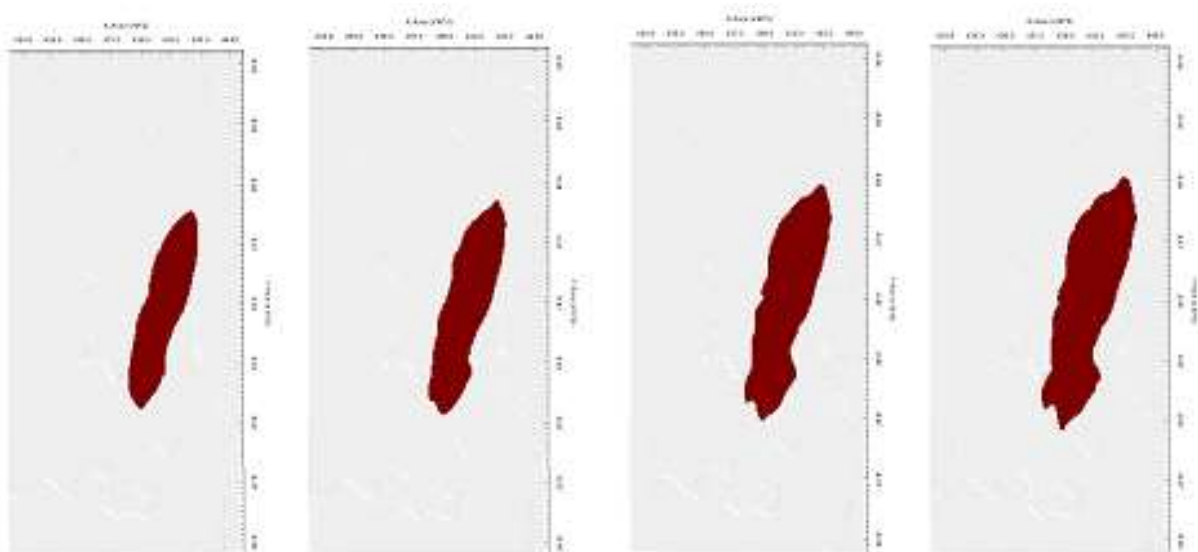


Figure 6: “Realistic” case simulation - plume prediction for 30yr, 50yr, 100yr and 200 yr of injection

However, in order to quantify leakage rates at the seafloor we continued injecting CO<sub>2</sub> for an unrealistic long period. Figure 7 shows that the CO<sub>2</sub> reaches the chimney structures after 110 years and starts to escape through the chimney to the seafloor.

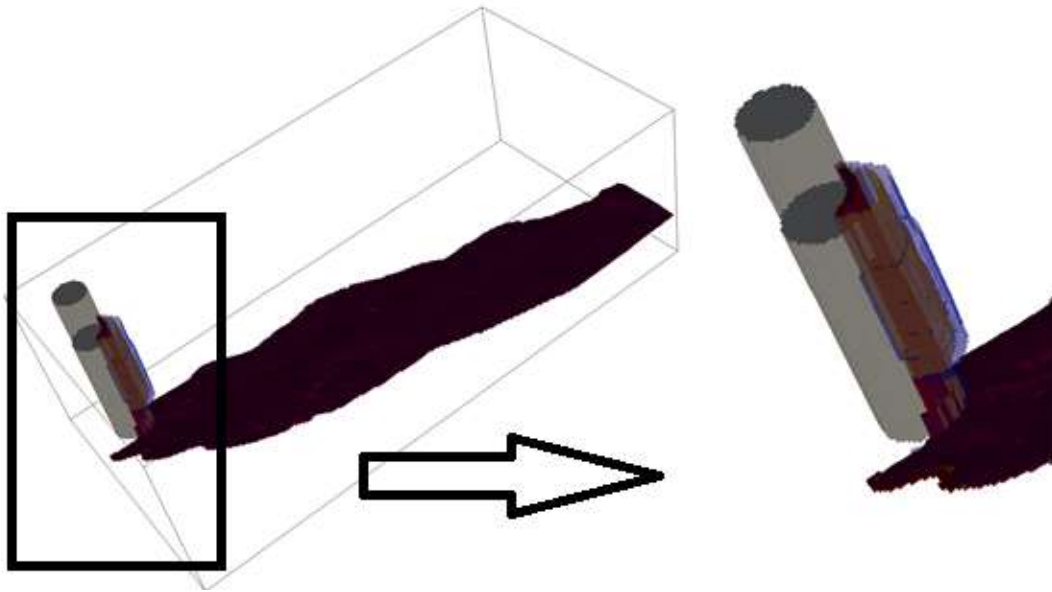


Figure 1: “Worst” case simulation – CO<sub>2</sub> plume migration with leakage along a chimney.

This scenario was simulated for different chimney permeabilities (Figure 8). This simulation showing that this parameter delays leakage, but does not change its magnitude.

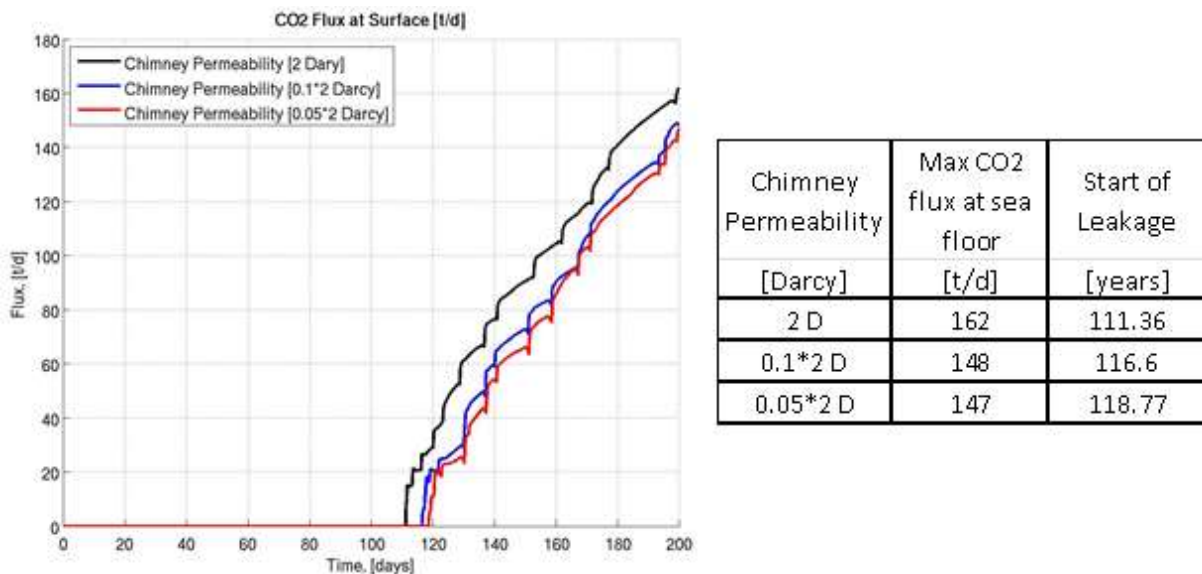


Figure 2: CO<sub>2</sub> flux at the surface for different chimney permeabilities

### 2.3. Fluid flow simulations of leakage along a elongated fluid conduit: Leakage along a fault at Snøwhit

The simulations involved injection over a 20 year period at a rate of 0.7 Mt/year and migration over a 2000 year time frame for domains of approx. 21 Km<sup>2</sup> for the sedimentary overburden fault models, see figure 3 below, in a layered sedimentary succession. The total mass of CO<sub>2</sub> injected in the reservoir during the total duration of the 20 year injection period is 14 Mt.

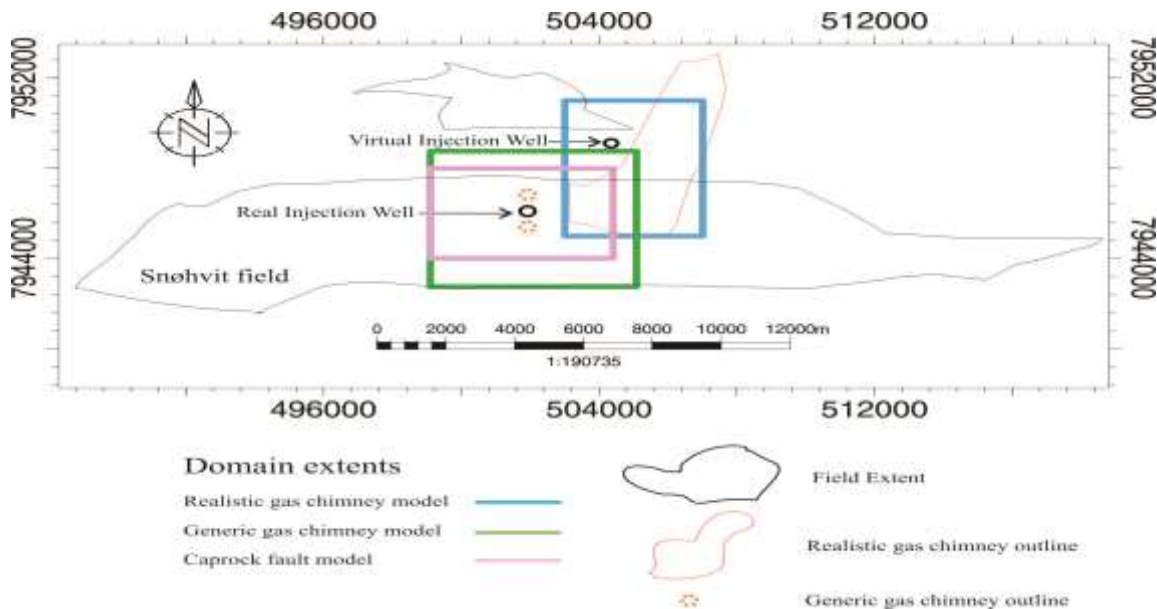


Figure 9: Domain extents for the 3 types of modeling groups, namely realistic and generic gas chimney models, sedimentary overburden fault models and location of modeled gas chimneys.

We built faulted models containing only 4 zones (the sedimentary cover, one zone above and the 2 reservoir zones below the sedimentary cover) because the CO<sub>2</sub> does not take the fault as a flow path due to too coarse grid resolution (Figure 1 above). We decided to ignore the overburden in the new grids that were built. The flux was measured only at 2300m, i.e. at the top of the sedimentary overburden. The faulted sedimentary cover geological model covers an area of about 21.1 Km<sup>2</sup> and reaches -2771 meters in depth (Figure 9). Its cell resolution in the horizontal plane is 25 meters by 25 meters and 17.68m in the vertical plane. In the faulted sedimentary cover scenarios background permeability, fault thickness and fault permeability were the parameters chosen to be varied. In the faulted sedimentary

ECO2 project number: 265847

Deliverable number 1.3, WP1, lead beneficiary no 1 (GEOMAR)

overburden scenarios CO<sub>2</sub> is injected into the Tubåen Formation, located in zone 9 of the models, at the realistic injection point one, corresponding to the real location of the CO<sub>2</sub> injection well, located at about 2600 meters below the upper grid boundary (Figure 9).

The study gave us a better idea of the parameters affecting the migration process of CO<sub>2</sub>, to what degree they do so and how sensitive these parameters are to any changes. In the following 2 simulations we observe the variation of the CO<sub>2</sub> plume distribution for 2 different scenarios considered. It's obvious from the 2 figures below that the background permeability has a clear effect on the CO<sub>2</sub> plume distribution. A lower background K makes CO<sub>2</sub> accumulate in the reservoir at 50 years after injection.

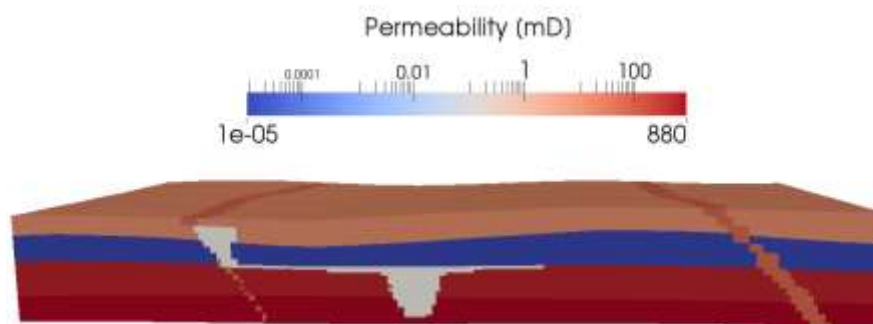


Figure 10: CO<sub>2</sub> plume distribution after 50 years within the **high** background permeability field (Fault thickness: 50m, fault permeability 50mD, Scenario F8).

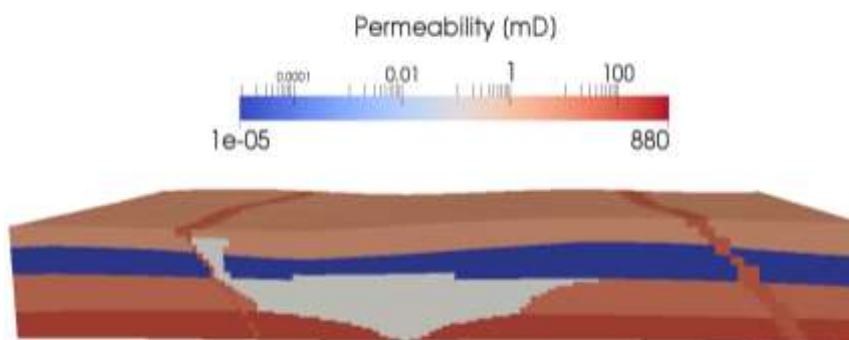


Figure 11: CO<sub>2</sub> plume distribution after 50 years within the **low** background permeability field (Fault thickness: 50m, fault permeability 50mD, Scenario F14).

For the worst case scenarios (Sc. F19, see faulted sedimentary overburden scenarios table above) it only takes 3.5 years, after start of injection, for CO<sub>2</sub> to start to leak (leakage was measured at 2300m depth which corresponds to the top of the sedimentary cover at Snøhvit). There is no leakage at the seabed for the faulted sedimentary cover scenarios.

## 2.4. Generic chimney Simulations - Formation of focused fluid flow structures as the result of CO<sub>2</sub> storage

The storage of CO<sub>2</sub> may create focused fluid flow structures due to blowout events. The generic chimney simulations aim to simulate the flow along such structures, but not the process of formation. For this purpose, generic chimneys were placed in the direct vicinity of the injection point to measure the near-field effect of high permeable fluid conduits.

The generic gas chimney geological models cover an area of about 35.4 Km<sup>2</sup> and reach -2804 meters in depth (Figure 12). Their cell resolution in the horizontal plane is 50 meters by 50 meters and 48.15m in the vertical plane.

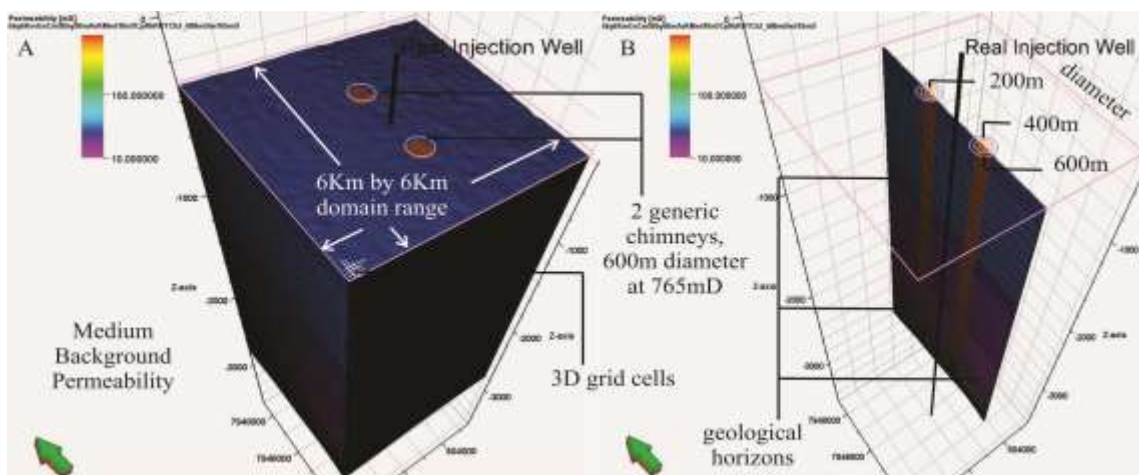


Figure 12: Generic chimney scenarios: Permeability model for the generic gas chimney scenario G3 (Medium background permeability, 2 generic gas chimneys of 600m diameter and at 765mD and 5B: cross section through the 2 generic gas chimneys.

The scenarios here contain either one or two round generic chimneys, 1Km away from the real injection site either to the north and/or to the south of it (Figures 5 and 6 below). Besides the background permeability (Low, Medium, High) (see MS12 geological models report), the chimney permeability (342, 765 to 3000mD), and the chimney width (200, 400 to 600m) are varied. For both the chimneys and the rest of the model we use the Medium scenario background porosity values (see MS12 geological models report).

The blowout scenario is summarized in more detail by the following graphs and characteristics:

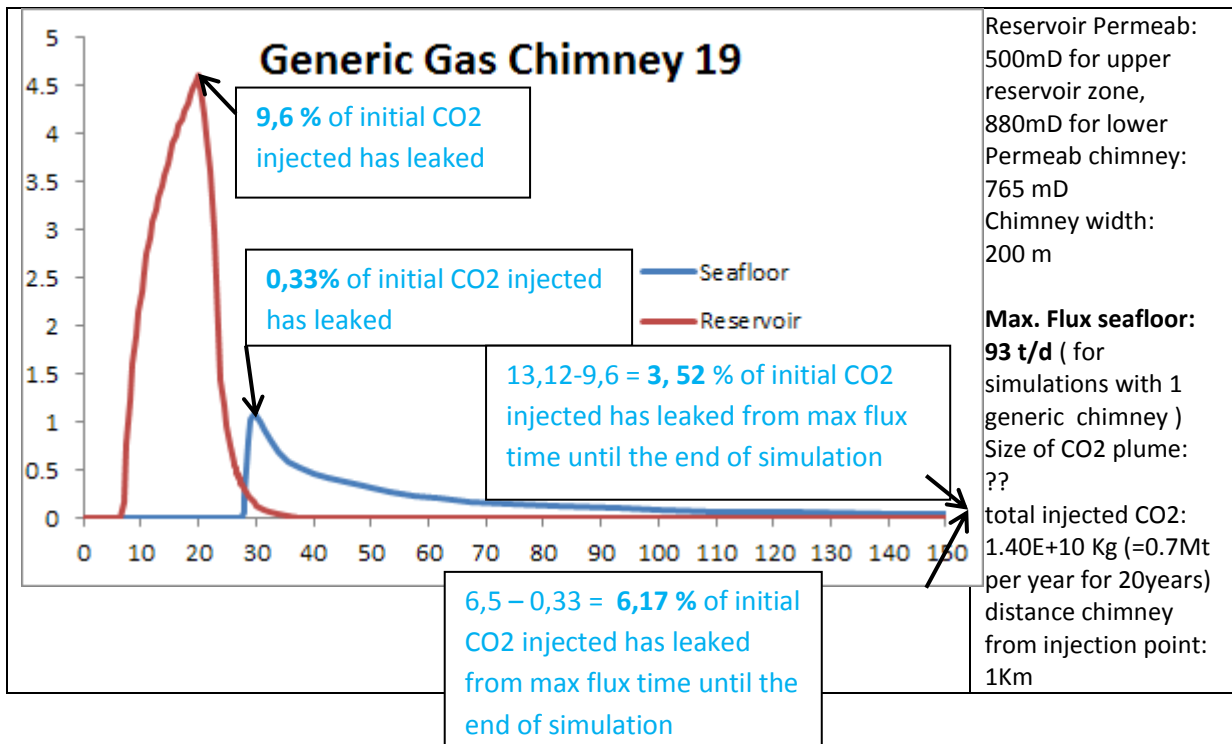


Figure 13: CO<sub>2</sub> flux simulation for the blowout scenario with most important model parameters.

## 2.5. Geomechanical simulation

CO<sub>2</sub> injection into saline aquifers will cause a pressure build-up in the storage formation, which in turn will change the state of stress in a reservoir-seal system. As a result of induced poro-mechanical stresses, and possibly thermal effects associated with injection of cold CO<sub>2</sub> into a hot storage formation, reservoir seals can be mechanically damaged and pre-existing sealing faults re-activated, creating pathways for fluid migration out of the storage complex (Hawkes et al., 2005; Orlic et al., 2011; Rutqvist, 2012). The geomechanical processes therefore play a key role in creating and opening the leakage pathways through reservoir seals, which connect the storage reservoir with the shallow overburden, either by reactivating and opening of the existing faults and fractures, or by creating the new ones.

The site-specific models developed by University of Tromsø (UiT) and the leakage scenario simulated by University of Stuttgart were analyzed and then used as a basis for developing geomechanical models. We focused on the leakage scenarios with faults and fractures as flow rates through these features are sensitive to the in situ stress regime and stress perturbations. Faults and fractures represent the common leakage pathways for natural

migration of fluids in the subsurface. The site-specific leakage scenarios simulated by University of Stuttgart could not be used in this context for geomechanical numerical analysis because the Sleipner leakage scenarios did not include leaking faults while in the Snøhvit fault leakage scenarios the leakage through permeable faults could not be observed in flow simulations (D1.1, 2012). Geomechanical simulations were conducted on the generic leakage model Fault 1 (described in detail in D1.1, 2012) with the objective to assess the geomechanical effects of CO<sub>2</sub> injection causing pressure build-up in the reservoir and the leaking fault zone.

The generic fault leakage scenario Fault 1 is used to simulate injection of 1 Mt/y of CO<sub>2</sub> in a 100m-thick, horizontal reservoir at a depth of 900 m (reservoir top; Figure 14a). The leakage feature implemented in this scenario is a 10m-thick vertical fault zone, located 500 away from the injection well. The vertical plane which connects the injection well and the leaky fault zone is a plane of symmetry; hence, only one-half of the model domain was simulated. The predicted maximum pressure increase in the reservoir, at the end of CO<sub>2</sub> injection period, is less than 20 bar (Figure 14b).

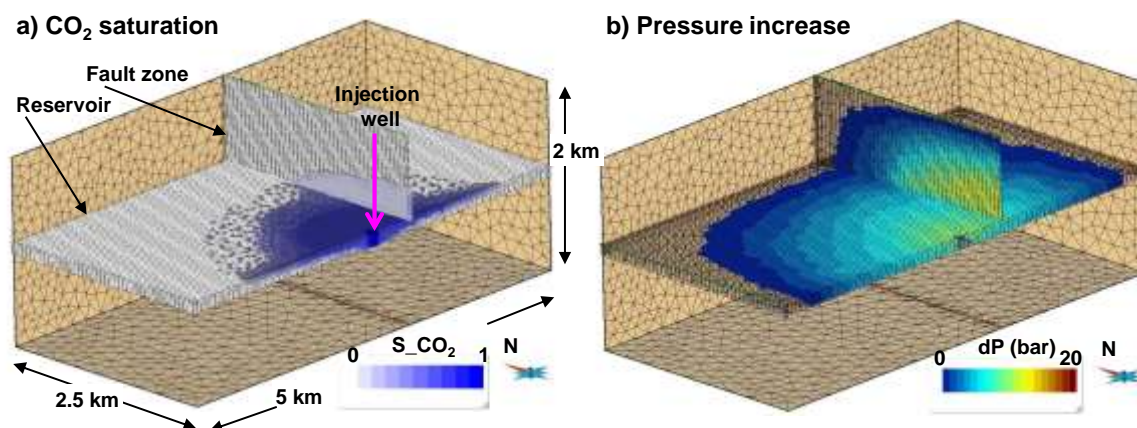


Figure 14: The generic leakage scenario Fault 1. a) CO<sub>2</sub> saturation distribution, and b) pressure build-up in the reservoir and the 10m-thick fault zone after 30 years of CO<sub>2</sub> injection (University of Stuttgart simulations; D1.1, 2012).

Geomechanical numerical model of the generic leakage scenario Fault 1 was developed using the general-purpose finite element package DIANA (TNO Diana, 2014). DIANA offers a wide range of constitutive models for geo-materials and frictional behaviour of faults. The mesh for the generic faulted model comprises 255,000 quadratic second-order ten-node

solid pyramid elements and 347,000 nodes (Figure 15a). Common structural boundary conditions were imposed on model boundaries to constrain displacements perpendicular to the sides and base of the model. The base case calculations were conducted assuming an isotropic elastic subsurface with an elastic modulus of  $E=18$  GPa and a Poisson's coefficient of  $\nu=0.18$  for the reservoir, surrounding rock and the fault zone. Transient pore pressures from DUMU<sup>X</sup> flow simulations were used as input loads for DIANA geomechanical simulator. A one-way hydro-mechanical coupling was used, assuming that pore pressure changes induce stress changes, while the induced stress changes do not influence transport properties and flow.

Linear elastic finite element analysis was used to assess the geomechanical stress changes and the associated deformation caused by pressure build-up. As a result of induced poro-mechanical stresses, the reservoir slightly expands causing a ground-surface uplift of 2-3 mm (Figure 15a) and an uplift of up to 5 mm at the reservoir top (Figure 15b). Besides the reservoir, the pore pressure also increases in the 10m-thick fault zone, inducing the poro-mechanical stresses, which slightly inflate the fault zone. The most important is the change of stress in the direction normal to the fault surface, as this stress component directly controls the width of the fault zone and therefore the flow rate through it. The maximum change in the normal effective stress acting within the fault zone amounts to 1.2 MPa (Figure 16a) and the normal strain remains below 0.6 millistrains (Figure 16b). The corresponding change in the hydraulic aperture of the 10m-faulted zone of less than 6 mm is still too small to affect flow rates through the fault despite the cubic relation between the flow rate and the aperture. According to the cubic law, flow rates of a Newtonian fluid through a single fracture are proportional to the cube of aperture (Zimmerman *et al.*, 1991):

$$\mathbf{q} = -\frac{w_h^3}{12\eta} \nabla P$$

where  $q$  is the flow rate,  $w_h$  is the hydraulic aperture of a fracture,  $P$  is the fluid pressure and  $\eta$  is the dynamic viscosity of the fluid.

It should be noted that faults are generally complex zones consisting of a fault core (with sharp slipping surfaces and fault gouge) surrounded by a fault damage zone with fractures. The elastic properties of fault zones are generally heterogeneous showing a reduction in Young's modulus with increasing damage. Faulted rocks are characterized by extreme localization of slip and flow paths, which cannot be captured in detail in large-scale flow and geomechanical simulation models due to limitations in the number of grid cells that can be handled by typical simulators. Flow through discrete fracture sets is therefore often simulated using a continuum approach: the fine scale (fracture) permeability is upscaled to coarse grid cells with the average transport properties equivalent to those of the fracture set. Such an approach is adequate for simulating average flow rates through the existing leaky faults and fracture zones. However, pressure build-up in localized faults/fractures may be underestimated, which could lead to underestimation of the related geomechanical effects. The conclusions which can be drawn from the geomechanical simulations of the generic leakage scenario Fault 1 that the geomechanical effects related to CO<sub>2</sub> injection are weak, are therefore not generally valid. Furthermore, for simulation of the dynamic geomechanical processes such as fault/fracture initiation, shear slip and fracture opening/closing, fine-scale coupled flow-stress models need to be developed, which can better capture the localized geomechanical processes and the associated permeability changes relevant for estimating variation of leakage rates over time.

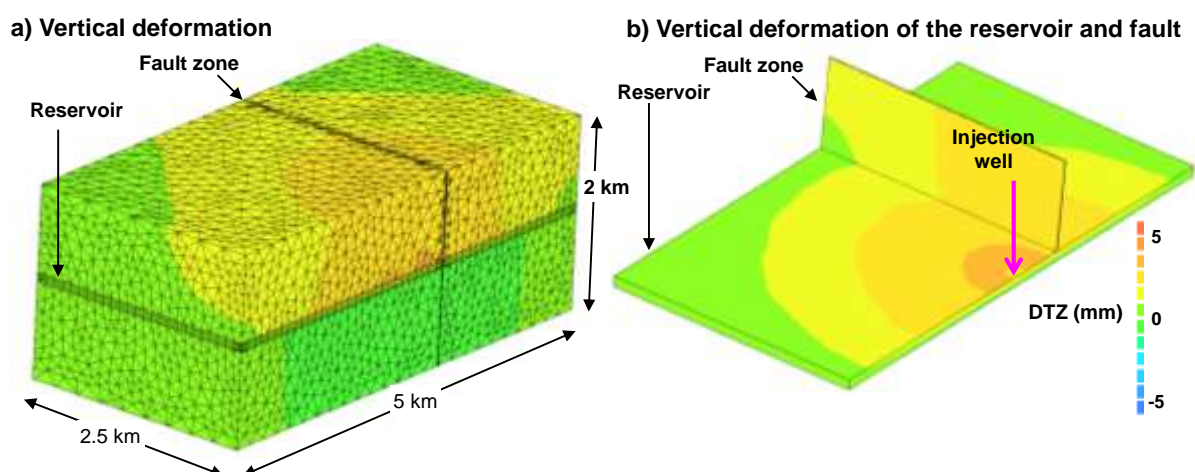


Figure 15: The generic leakage scenario Fault 1. Induced vertical deformation in a) the whole model, and b) the reservoir and the fault zone. Positive sign indicates uplift.

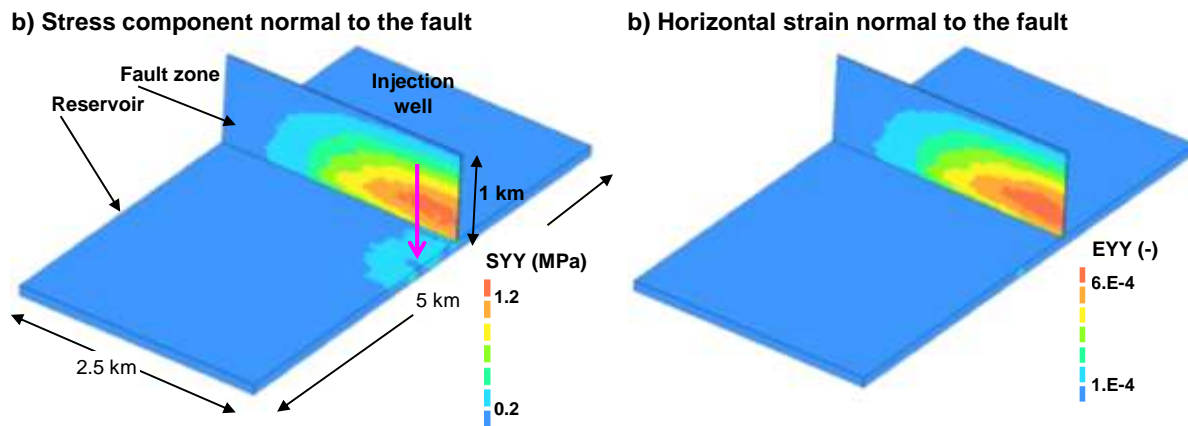


Figure 16. The generic leakage scenario Fault 1. Changes in a) the normal effective stress, and b) the normal strain within the fault zone. Positive sign indicates unloading, i.e. decrease in the (compressive) normal stress acting in the fault zone, and dilation of the fault zone.

### 3. Summary and recommendations

Assessing the risks for CO<sub>2</sub> leakage from a sub-seabed sequestration site is a complex task, which requires detailed knowledge about local geology including the natural fluid flow system and the hydraulic parameters of the seal and the storage formation. The results of the ECO2 project could illustrate that the reconstruction of the local fluid system requires the usage of different geophysical and geological survey methods. The best example for this is the Hugin fracture, which could only be identified by the usage of high resolution AUV surveys, while it is not visible in conventional 3D seismic data. The large chimney structures, which most likely represent inactive fluid conduits, did not show any prominent seafloor anomaly. This proves the importance of multi methodological and, in case of acoustic surveys, multi-frequency approaches to address their different sensitivities.

In order to understand the relevance of specific potential leakage structures, it is necessary to integrate them into geological models, which are the base geomechanical and fluid flow simulations. The simulations conducted within the framework of the ECO2 project revealed that only very little is known about the hydraulic properties of focused fluid conduits. Nevertheless, it was possible to achieve valuable results about their potential influence on the long-term performance of geological storage sites and leakage parameters.

**ECO2 project number: 265847**

**Deliverable number 1.3, WP1, lead beneficiary no 1 (GEOMAR)**

Future leakage assessment activities have to focus on quantifying the hydraulic properties of seal by-passing fluid conduits by studying field analogues, using multi-frequency acoustic surveys and ideally drilling into these structures. Only a detailed knowledge about the hydraulic properties may help to quantify their actual leakage potential and how to integrate them in monitoring strategies.

WP1 has investigated the geological processes that act on the overburden from many different angles and with a multitude of methods. There are two important findings for risk assessment of CCS projects.

The first conclusion that we can draw is that there is a fundamental lack of understanding of the seismic anomalies that penetrate vertically sedimentary basins for several 1000 m. We have taken great care within this project to compile all the published information on their physical properties and we have carefully analyzed the seismic characteristics of such structures. But we have shown that unless the bulk permeability of these structures is better constrained by drilling and laboratory experiments large uncertainties remain how they affect the hydrological systems and seepage predictions cannot be reliable in areas with such seismic anomalies until future projects have studied this in detail.

The second conclusion that we draw is that it is mandatory to have high-quality 3D seismic data available when assessing the geological risks. The studies at Snøhvit and Sleipner have documented impressively that only with high-quality 3D seismic data coverage between the injection point and the surface there is a chance of getting a handle on the overburden geology and link sea floor observations to the injection of CCS.

### **Acknowledgement**

This project has received funding from the European Union's Seventh Framework Programme for research; technological development and demonstration und grant agreement n° 265847.

#### 4. References

Cartwright, J., Huuse, M., Aplin, A., 2007. Seal bypass systems. Bulletin 91, 1141–1166.

ECO<sub>2</sub> Deliverable report D1.1, 2012. *Report of Leakage Assessment*.

Hawkes, C., McLellan, P.J., Zimmer, U., Bachu, S., 2005. Geomechanical factors affecting geological storage of CO<sub>2</sub> in depleted oil and gas reservoirs: risks and mechanisms, *Journal of Canadian Petroleum Technology*, 44: 52-61.

Janssen, C., Wirth, R., Reinicke, A., Rybacki, E., Naumann, R., Wenk, H.R., Dresen, G., 2011. Nanoscale porosity in SAFOD core samples (San Andreas Fault). *Earth Planet Sc Lett* 301, 179-189.

Karstens, J., and Berndt, C., 2015. Seismic chimneys in the Southern Viking Graben – Implications for palaeo fluid migration and overpressure evolution. *Earth and Planetary Science Letters*, v. 412, pp. 88-100.

Løseth, H., Gading, M., Wensaas, L., 2009. Hydrocarbon leakage interpreted on seismic data. *Marine and Petroleum Geology* 26, 1304–1319.

Løtveit, F.I., Gudmundsson, A., Sydnes, M., 2012. How the stress changes due to glacial erosion may have caused leakage of hydrocarbons in the SW Barents Sea. Arctic Frontiers Conference Presentation.

Mizoguchi, K., Hirose, T., Shimamoto, T., Fukuyama, E., 2008. Internal structure and permeability of the Nojima fault, southwest Japan. *J Struct Geol* 30, 513-524.

Moore, D.E., Lockner, D.A., Ito, H., Ikeda, R., Tanaka, H., Omura, K., 2009. Geometry of the Nojima Fault at Nojima-Hirabayashi, Japan - II. Microstructures and their Implications for Permeability and Strength. *Pure Appl Geophys* 166, 1669-1691.

Ostanin, I., Anka, Z., di Primio, R., Bernal, A., 2013. Hydrocarbon plumbing systems above the Snohvit gas field: Structural control and implications for thermogenic methane leakage in the Hammerfest Basin, SW Barents Sea. *Mar Petrol Geol* 43, 127-146.

Orlic, B., ter Heege, J., Wassing, B.B.T., 2011. Assessing the short-term and long-term integrity of top seals in feasibility studies of geological CO<sub>2</sub> storage, *Proceedings of the 45<sup>th</sup> US Rock Mechanics / Geomechanics Symposium (ARMA)*, San Francisco, paper no ARMA 11-375.

**ECO2 project number: 265847**

**Deliverable number 1.3, WP1, lead beneficiary no 1 (GEOMAR)**

Ostanin, I., Anka, Z., Primio, R.D., Bernal, A., 2012. Identification of a large Upper Cretaceous polygonal fault network in the Hammerfest basin: Implications on the reactivation of regional faulting and gas leakage dynamics, SW Barents Sea. *Marine Geology*

Petersen, C.J., Bunz, S., Huston, S., Mienert, J., Klaeschen, D., 2010. High-resolution P-Cable 3D seismic imaging of gas chimney structures in gas hydrated sediments of an Arctic sediment drift. *Marine and Petroleum Geology* 27, 1981-1994.

Planke, S., Eriksen, F.N., Berndt, C., Mienert, J., Masson, D., 2009. P-Cable High-Resolution Seismic. *Oceanography* 22, 85-85.

Rajan, A., Bunz, S., Mienert, J., Smith, A.J., 2013. Gas hydrate systems in petroleum provinces of the SW-Barents Sea. *Marine and Petroleum Geology* 46, 92-106.

Rotevatn, A., Sandve, T.H., Keilegavlen, E., Kolyukhin, D., Fossen, H., 2013. Deformation bands and their impact on fluid flow in sandstone reservoirs: the role of natural thickness variations. *Geofluids* 13, 359-371.

Rutqvist, J., 2012. The geomechanics of CO<sub>2</sub> storage in deep sedimentary formations, *Geotechnical and Geological Engineering*, 30(3):525-551.

TNO Diana, 2014. *DIANA: Finite element program and User Documentation*, version 9.5 ([www.tnodiana.com](http://www.tnodiana.com)).

Zimmerman, R.W., Kumar, S., Bodvarsson, G.S., 1991. Lubrication theory analysis of the permeability of rough-walled fractures, *International Journal of Rock Mechanics and Mining Sciences & Geomechanics Abstracts*, 28(4), 325-331.